arXiv:2001.07743v1 [quant-ph] 21 Jan 2020

Strong Spin-Orbit Quenching *via* the Product Jahn-Teller Effect in Neutral Group IV Artificial Atom Qubits in Diamond

Christopher J. Ciccarino,[1,2,*] Johannes Flick,[1,3,*] Isaac B. Harris,[1,4]
Matthew E. Trusheim,[1] Dirk R. Englund,[4] and Prineha Narang[1,†]

[1]*John A. Paulson School of Engineering and Applied Sciences, Harvard University, Cambridge, MA, USA*
[2]*Department of Chemistry and Chemical Biology, Harvard University, Cambridge, MA, USA*
[3]*Center for Computational Quantum Physics, Flatiron Institute, New York, NY, USA*
[4]*Department of Electrical Engineering and Computer Science, Massachusetts Institute of Technology, Cambridge, MA, USA*

(Dated: January 24, 2022)

Artificial atom qubits in diamond have emerged as leading candidates for a range of solid-state quantum systems, from quantum sensors to repeater nodes in memory-enhanced quantum communication. Inversion-symmetric group IV vacancy centers, comprised of Si, Ge, Sn and Pb dopants, hold particular promise as their neutrally charged electronic configuration results in a ground-state spin triplet, enabling long spin coherence above cryogenic temperatures. However, despite the tremendous interest in these defects, a theoretical understanding of the electronic and spin structure of these centers remains elusive. In this context, we predict the ground- and excited-state properties of the neutral group IV color centers from first principles. We capture the product Jahn-Teller effect found in the excited state manifold to second order in electron-phonon coupling, and present a non-perturbative treatment of the effect of spin-orbit coupling. Importantly, we find that spin-orbit splitting is strongly quenched due to the dominant Jahn-Teller effect, with the lowest optically-active ^3E_u state weakly split into m_s-resolved states. The predicted complex vibronic spectra of the neutral group IV color centers are essential for their experimental identification and have key implications for use of these systems in quantum information science.

Artificial atoms in diamond are promising candidates for a wide variety of quantum technologies,[1–5] including as quantum repeaters for long-range quantum networks.[6,7] Many milestones have been reached using the nitrogen-vacancy (NV^-) center[8,9] and more recently the SiV^-.[10–14] Further exploration of novel defect candidates has included the GeV^-,[15–18] SnV^-,[19–22] PbV^-[23,24] and SiV^0,[25–27] all of which have been observed experimentally and described theoretically.[28,29] The neutrally-charged SiV^0 has symmetry analogous to the SiV^-, but its missing electron gives rise to a triplet ground state as found in the NV^-, with the corresponding potential for both long spin coherence times and symmetry-protected optical transitions. Theoretical work has postulated the remaining group IV neutral (IV^0) centers[29] (GeV^0, SnV^0, PbV^0) and described the negatively-charged group III defect centers[30] as isoelectronic to the SiV^0. Calculations suggest that all of these defect candidates are thermodynamically more likely to exist in intrinsic diamond than the SiV^0, which requires p-type doping.[27] Within this growing space of candidate artificial atom qubits, an *ab initio* understanding of the level structure is required to harness the advantages of each emitter in quantum science.[31]

Accurate descriptions of artificial atoms in diamond can be particularly challenging because of the dominant Jahn-Teller (JT) distortions[32] present. In such systems, the total energy of a JT-unstable electronic configuration is lowered as a result of the coupling of the electronic structure to nuclear motion, introducing electron-phonon interactions. In the case of group IV^0 defects, the excited state exhibits a product Jahn-Teller (pJT) effect which results from simultaneous Jahn-Teller instabilities in two orbitals.[29,33–35] The pJT interaction leads to either a dynamical or static JT effect, or a mixture of both. In the case of a dynamical JT distortion, the system is best described as a collective electron-vibration (vibronic) system. This strong coupling of electronic and vibrational states may modify electronic observables, for example a quenching of spin-orbit (SO) coupling (SOC).

Including the pJT effect is therefore critical for predictions of the zero-phonon line (ZPL) transition energies and the excited-state level structure. Previous work has found that describing pJT interactions to first order in coupling explains the observed energy splitting[25] between the optically-bright E_u and dark A_{2u} states for SiV^0.[29] An important effect to consider, particularly for the heavier group IV^0 defects, is the role of spin-orbit interactions, as these defects can have coupling constants on the order of 100s of meV.[28] The interplay of SOC interactions and JT physics in the excited-state of group IV^0 centers has significant impact on the expected SO behavior if the JT effect couples the electrons and phonons strongly, as we find.

In this *Letter*, we describe the combined impact of spin-orbit and Jahn-Teller interactions in the neutral group IV centers in diamond from first principles. We describe the product Jahn-Teller effect to second order in electron-phonon coupling and find a large second order energy shift. Importantly, the effects of spin-orbit coupling are included non-perturbatively and splittings are found to be an order of magnitude smaller than expected for a purely electronic system as a result of the JT interaction. These fine structure details reveal new physics of color center qubits in diamond and present a pathway to identify GeV^0, SnV^0 and PbV^0 experimentally.

The group IV centers in diamond adopt a split-vacancy configuration within the diamond lattice where the dopant

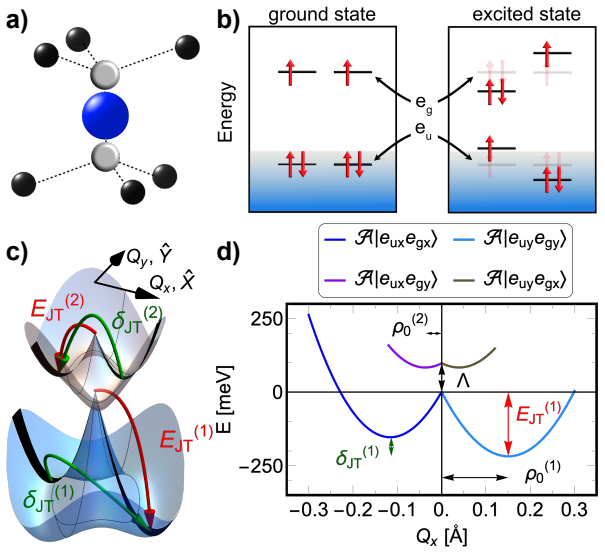


FIG. 1. **(a)** Lattice configuration of the group IV^0 defects, in which the impurity atom (blue) sits between two vacant carbon sites (grey). **(b)** Simplified energy level diagram showing the energy location of the doubly-degenerate e_u and e_g orbitals relative to the band gap of bulk diamond. The ground state is a spin triplet and the corresponding excited state undergoes a symmetry-breaking pJT distortion (right) as a result of orbital instabilities in both the e_u and e_g orbitals. **(c)** Potential energy surfaces computed for the pJT system including effects up to 2$^{\text{nd}}$ order in coupling. Here we label the energy instability by $E_{\text{JT}}^{(i)}$ for the result of constructive ($i = 1$) and destructive ($i = 2$) interference of the two orbital branches. The axial asymmetry arises from a second order effect denoted similarly by the parameter $\delta_{\text{JT}}^{(i)}$. The black curves indicate 1D cuts through the 2D (Q_x, Q_y) distortion space which allows us to fully parameterize the system. **(d)** DFT-obtained potential energy surfaces along these 1D cuts for the SnV^0 defect. The D_{3d} high-symmetry point ($Q_x = 0$ Å) is found to be unstable in two surfaces, consistent with the pJT picture. We also label the displacement amplitudes $\rho_0^{(i)}$ from the D_{3d} to the C_{2h} minima. The splitting Λ is a result of static electronic correlation. All values are tabulated in Table I.

group IV atom sits between two vacant carbon sites, as shown in Fig. 1(a) and denoted by the point group D_{3d}. The defect introduces localized electronic orbitals comprised of the dangling bonds of the nearby carbon atoms, which can be captured using density functional theory (DFT)[36] (see SI for computational details) and are labeled by their symmetry. The energetically-relevant orbitals are of e_u and e_g character and exist near and above the valence band of intrinsic diamond, respectively, shown schematically in Fig. 1(b). Both the e_u and e_g orbitals are doubly-degenerate and can be further labeled by their spatial orientation, i.e., $\{e_u\} = \{e_{ux}, e_{uy}\}$ and similarly $\{e_g\} = \{e_{gx}, e_{gy}\}$. Including spin, these levels combined can host up to eight electrons. For group IV^0 centers, six electrons are present in the $(e_u e_g)$ manifold. Equivalently, we can describe these electronic states in the basis of two defect-bound holes. We choose to adopt this convention for the remainder of this *Letter*.

The ground state has the hole configuration e_g^2 $(e_{gx}^1 e_{gy}^1)$, and prefers the triplet $S = 1$ spin configuration. The total defect wavefunction is of $^3A_{2g}$ symmetry, and is directly obtained from electronic structure calculations. In constructing the total wavefunction, given the symmetric triplet spin component, we ensure that the orbital wavefunction is antisymmetrized; this is given by the $\mathcal{A}$ symbol. The ground state orbital wavefunction can be written as $\mathcal{A}|e_{gx}e_{gy}\rangle = 1/\sqrt{2}\left(e_{gx}(\mathbf{r}_1)e_{gy}(\mathbf{r}_2) - e_{gx}(\mathbf{r}_2)e_{gy}(\mathbf{r}_1)\right)$. In the excited electronic configuration, one hole moves from an e_g to an e_u orbital. Unlike in the ground state, there exist four distinct hole occupations with this $e_g^1 e_u^1$ configuration. The antisymmetrized orbital wavefunctions are given by $\mathcal{A}|e_{ux}e_{gx}\rangle$, $\mathcal{A}|e_{uy}e_{gx}\rangle$, $\mathcal{A}|e_{ux}e_{gy}\rangle$, and $\mathcal{A}|e_{uy}e_{gy}\rangle$. We can construct the irreducible representations of the triplet subspace as linear combinations of these orbital states, as has been done previously.[29]

Each of these antisymmetrized states obtained from our *ab initio* calculations are Jahn-Teller unstable, in that they energetically prefer a configuration with the lower symmetry C_{2h} point group to that with the higher symmetry D_{3d} point group. The nuclear motion associated with these distortions is a result of interactions with phonon modes of symmetry E_g. In contrast with the single JT system ($E_g \otimes e$), the JT distortion found in the excited state of group IV^0 systems is due to simultaneous JT interactions in both the e_u and e_g orbitals. This collective product Jahn-Teller behavior is denoted by $E_g \otimes e_u \otimes e_g$ and shown schematically in the right panel of Fig. 1(b). Previous work has covered the single JT to second order as well as the pJT[32,33,35] to first order in electron-phonon coupling. Here, we describe the coupling of the two electronic states with the E_g-type vibrational mode to second order in vibrational coupling. The Hamiltonian for this interaction can be written as:

$$\begin{aligned}\hat{\mathrm{H}}_{\text{pJT}}^{(2)} =& F_u\left(\hat{X}\hat{\sigma}_z \otimes \hat{\sigma}_0 - \hat{Y}\hat{\sigma}_x \otimes \hat{\sigma}_0\right) \\ &+ F_g\left(\hat{X}\hat{\sigma}_0 \otimes \hat{\sigma}_z - \hat{Y}\hat{\sigma}_0 \otimes \hat{\sigma}_x\right) \\ &+ G_u\left(\left(\hat{X}^2 - \hat{Y}^2\right)\hat{\sigma}_z \otimes \hat{\sigma}_0 + 2\hat{X}\hat{Y}\hat{\sigma}_x \otimes \hat{\sigma}_0\right) \\ &+ G_g\left(\left(\hat{X}^2 - \hat{Y}^2\right)\hat{\sigma}_0 \otimes \hat{\sigma}_z + 2\hat{X}\hat{Y}\hat{\sigma}_0 \otimes \hat{\sigma}_x\right). \quad (1)\end{aligned}$$

The first two lines represent linear coupling with coupling constants $F_{u/g}$ while the latter two represent quadratic coupling terms with coupling constants $G_{u/g}$ for both the e_g and e_u orbital branches. The nuclear component of the Hamiltonian is written with $\hat{X}$ and $\hat{Y}$ representing bosonic operators for the phonons given by $\{\hat{X}, \hat{Y}\} = (\hat{a}^\dagger_{\{x,y\}} + \hat{a}_{\{x,y\}})/\sqrt{2}$ and the electronic component in terms of $\hat{\sigma}_i$ which are the standard Pauli and unit matrices acting on the $e_u \otimes e_g$ subspace. The Hamiltonian in Eq. 1 is defined within the single-excitation 2-particle hole manifold, therefore the basis states are $\mathcal{A}|e_{ux}e_{gx}\rangle$, $\mathcal{A}|e_{uy}e_{gx}\rangle$, $\mathcal{A}|e_{ux}e_{gy}\rangle$, and $\mathcal{A}|e_{uy}e_{gy}\rangle$, which are captured from electronic structure calculations.

In the pJT case, two independent solutions which are unstable at the high-symmetry point can exist. One corresponds to the constructive interference of the two JT distortions ($\sim (F_g + F_u)^2$) and the other to the destructive interference ($\sim (F_g - F_u)^2$), as shown in Fig. 1(c). To find the coupling constants and solve for the coupled vibronic states, we obtain displacement $\rho_0^{(i)}$ and energy $E_{\mathrm{JT}}^{(i)}$, $\delta_{\mathrm{JT}}^{(i)}$ parameters from the defect potential energy surfaces (PES) computed from first principles electronic structure, where $i = 1, 2$ for the constructive and destructive pJT, respectively. For the SnV^0 color center we show the resulting adiabatic PES as a one-dimensional cut along $Q_y = 0$ in Fig. 1(d). In principle the PES are two-dimensional, with the minima being threefold degenerate (see Fig. 1(c)). However, due to the symmetry of the PES, this 1D cut completely parameterizes the pJT Hamiltonian. For additional details on connecting the coupling constants in Eq. 1 to our calculations, refer to the SI.

In these defect systems electronic correlation $\hat{\mathrm{W}}$ plays a role in splitting the electronic states for reasons distinct from the Jahn-Teller physics. This correlation can be incorporated along the lines of previous work,[29] leading to the following total Hamiltonian for the system:

$$\hat{\mathrm{H}} = \hat{\mathrm{H}}_{\mathrm{osc}} + \hat{\mathrm{H}}_{\mathrm{pJT}}^{(2)} + \hat{\mathrm{W}}. \tag{2}$$

Here, $\hat{\mathrm{H}}_{\mathrm{osc}} = \hbar\omega_E \sum_{i=x,y} \left(\hat{a}_i^\dagger \hat{a}_i + 1/2\right)$ is the two-dimensional harmonic oscillator Hamiltonian for the E_g phonon modes of energy $\hbar\omega_E$.

Next we describe spin-orbit interactions in the pJT system. In the presence of a dynamical JT effect, expectation values of purely electronic operators can be quenched because of the coupled vibronic nature of the system, as first shown by Ham.[37] Thus it is important to analyze the effects of SO interactions with caution, as has already been demonstrated for the group IV^- defects.[28] In these group IV^0 centers, the SOC Hamiltonian can be written as a product of the single-hole interactions,[38] since the spin-orbit coupling does not mix the e_u and e_g orbitals.[39] The SOC Hamiltonian is written as

$$\hat{\mathrm{H}}_{\mathrm{SOC}} = m_s \left(\frac{\lambda_u^0}{2} (\hat{\sigma}_y \otimes \hat{\sigma}_0) + \frac{\lambda_g^0}{2} (\hat{\sigma}_0 \otimes \hat{\sigma}_y) \right). \tag{3}$$

Here, we introduce SO splittings $\lambda_{u/g}^0$ for both the e_u and e_g orbitals, which can be obtained from *ab initio* calculations. The variable m_s corresponds to eigenvalues of $\hat{S}_z$ and for the $S = 1$ triplet system can take on values of $m_s \in [1, 0, -1]$. While SOC in its general $\hat{\mathbf{L}} \cdot \hat{\mathbf{S}}$ form (with angular momentum operator $\hat{\mathbf{L}}$ and spin operator $\hat{\mathbf{S}}$) also contains transverse terms, these transverse terms only couple e_g/e_u orbitals to a_{2u} orbitals which are outside the (e_g, e_u) manifold of interest.[39] This consideration allows us to effectively write $\hat{\mathrm{H}}_{\mathrm{SOC}}$ solely in terms proportional to $\hat{L}_z \hat{S}_z$, yielding Eq. 3. The $\hat{L}_z \hat{S}_z$ interactions can couple the excited-state singlet manifold with the $m_s = 0$ excited-state triplets, however we choose to consider only the triplet subspace as the $(e_u^1 e_g^1)$ singlet excited states are expected to be higher in energy due to Coulomb repulsion.[26] Ultimately intersystem crossing (ISC) rates between these triplet and singlet levels will likely depend on phonon overlaps of the full diamond + defect system, however they require nonzero spin-orbit coupling and thus our analysis is important for further understanding ISC.

To capture the spin-orbit interaction in addition to the pJT physics, we find that including SOC perturbatively is insufficient, even for the SiV^0 system. Thus, we invoke a complete spin-resolved orbital basis including all spin sublevels of Eq. 3. From this we perform direct diagonalization of the combined spin-orbit and Jahn-Teller system (see SI), where we take all terms in Eq. 2 to be spin-independent. The solutions of this coupled Hamiltonian allows us to extract both the absolute energy shifts of our vibronic eigenstates with SO effects and the effective SO splittings between spin sublevels non-perturbatively.

Table I summarizes the results of our work. In each of the defect centers studied, we find a significant pJT effect, with the constructive interference yielding instabilities of over 200 meV. We find the second order effects are also relatively large, with $\delta_{\mathrm{JT}}^{(1)} \sim 0.3 E_{\mathrm{JT}}^{(1)}$ for each of the defects studied.

	SiV^0	GeV^0	SnV^0	PbV^0
$\rho_0^{(1)}$ [Å]	0.171	0.166	0.154	0.145
$\rho_0^{(2)}$ [Å]	-0.006	-0.022	-0.038	-0.051
$\hbar\omega_E$ [meV]	87.3	86.6	87.7	90.8
Λ [meV]	81.6	86.4	98.2	112.5
$E_{\mathrm{JT}}^{(1)}$ [meV]	258	244	217	200
$\delta_{\mathrm{JT}}^{(1)}$ [meV]	82.2	75.5	63.5	64.5
$E_{\mathrm{JT}}^{(2)}$ [meV]	0.289	4.61	14.9	29.9
$\delta_{\mathrm{JT}}^{(2)}$ [meV]	0.147	0.307	0.226	2.18
$\gamma^{(1)}$ [meV]	7.18	7.59	8.96	10.4
$\gamma^{(2)}$ [meV]	3.21	4.06	6.22	7.90
ZPL (^3E_u) [eV]	1.361	1.813	1.833	2.216
$\gamma^{(2)}$ + SOC [meV]	3.17	3.77	4.76	2.03
ZPL (^3E_u) + SOC [eV]	1.361	1.812	1.825	2.170
p_u	0.012	0.017	0.032	0.043
p_g	0.012	0.012	0.023	0.040
$\lambda_u + \lambda_g$ [meV]	0.089	0.622	3.15	11.31

TABLE I. We determine the parameters $\rho_0^{(i)}$, $E_{\mathrm{JT}}^{(i)}$, $\delta_{\mathrm{JT}}^{(i)}$ and Λ directly from the DFT potential energy surface (e.g., Fig. 1(d)). The effective vibrational energy $\hbar\omega_E$ can be found from these parameters similarly to the case of the single Jahn-Teller (see SI). The vibronic splitting between the lowest levels to first and second order are given by $\gamma^{(1)}$ and $\gamma^{(2)}$, respectively. SO effects are included non-perturbatively and we find significant quenching of the pure electronic SO splitting ($p_{u,g} \ll 1$), a consequence of the strong electron-phonon coupling induced by the pJT. The energy $\lambda_u + \lambda_g$ corresponds to the energy splitting between the $m_s = \pm 1$ levels of the lowest E_u vibronic eigenstates.

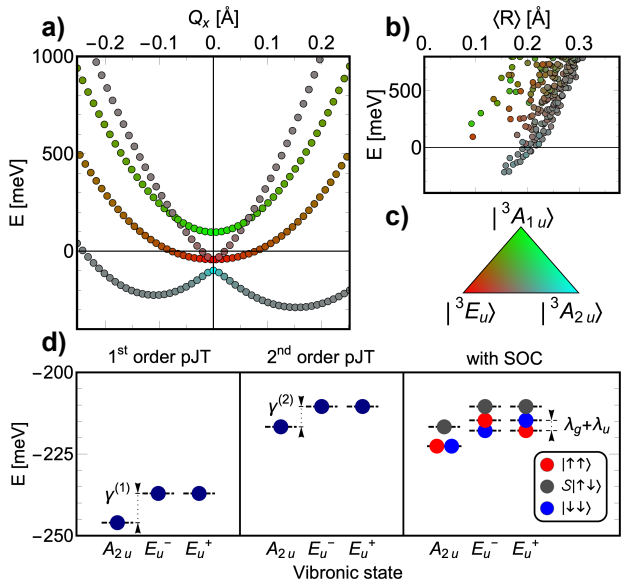


FIG. 2. **(a)** 1D cut ($Q_y = 0$) of the full electron-vibration coupled PES within the adiabatic approximation for SnV^0. **(b)** The vibronic eigenstates found after solving the pJT and electronic correlation Hamiltonian (Eq. 2), where the x-axis corresponds to the expectation value of the nuclear position coordinate $R = \sqrt{Q_x^2 + Q_y^2}$ relative to the D_{3d} minima. The solutions for both panels (a) and (b) are projected onto the D_{3d} symmetry-adapted electronic states and the resulting composition is represented by the color shown in **(c)**. **(d)** The effects of 2nd order JT and explicit inclusion of SOC are detailed for the lowest-energy eigenstates of the system. In 1st and 2nd order JT, the A_{2u} state is nondegenerate and the E_u state is twice degenerate. The inclusion of second order decreases the splitting γ between these levels, while also introducing an absolute energy shift of around 20 meV. The inclusion of SOC splits the E_u levels into E_u^+ and E_u^-, each with corresponding m_s sublevels. The splitting between the $m_s = \pm 1$ levels is given by $\lambda_g + \lambda_u$, which is strongly attenuated. The $m_s = 0$ (labeled by $|\mathcal{S}|\uparrow\downarrow\rangle$) levels are unaffected by SOC.

These second order shifts are important, as they represent the energy barrier between the three energy minima present in the 2D vibrational (Q_x, Q_y) space. This energy barrier helps to determine if the system will prefer a static or dynamic JT distortion, the latter of which means the electron and phonon degrees of freedom cannot be decoupled and instead a coupled vibronic solution is required. Indeed, the system can be parameterized as strongly-coupled as given by the parameter $\lambda = E_{\mathrm{JT}}/\hbar\omega_E$, which is > 2 for all cases studied here. After calculation of the parameters in Table I, we can solve for the coupled electron-vibrational system as defined in Eqs. 1 and 2.

Figure 2 visualizes our results for SnV^0. Panel (a) represents the adiabatic states along a 1D cut of the vibrational space with $Q_y = 0$. The full vibronic solutions to Eq. 2 are shown in panel (b), plotted as a function of the expectation value of displacement from the high-symmetry D_{3d} minima. In both cases we can project the solutions onto the irreducible states of the D_{3d} excited-state manifold, with the color legend given in panel (c). We find that the lowest energy states are comprised of roughly equal contributions from the undistorted $|^3E_u\rangle$ and $|^3A_{2u}\rangle$ electronic states. This is true for the quadratic coupling as well. In Fig. 2(d) we specifically focus on the lowest-energy vibronic solutions. The lowest vibronic state has total symmetry A_{2u} which is optically dark, whereas the next eigenstate is an optically-active, doubly-degenerate E_u level. In first order pJT, the splitting $\gamma^{(1)}$ between these two states for SnV^0 is 8.96 meV, while including second-order coupling decreases splitting $\gamma^{(2)}$ to just 6.22 meV. Even at second order, the ^3E_u state remains degenerate, however overall the eigenstates of the system shift upwards in energy by roughly 20 meV.

It is interesting to note that in general including second-order terms in the pJT Hamiltonian decreases the splitting γ between the lowest vibronic states (see Table I). This splitting was measured experimentally for SiV^0[25] to be 6.8 meV; here we find a larger discrepancy to experiment in the case of quadratic coupling ($\gamma^{(2)} = 3.2$ meV) than we do for linear coupling ($\gamma^{(1)} = 7.2$ meV). We emphasize, however, that an inclusion of second order electron-phonon coupling more closely resembles the *ab initio* data, as can be seen in Fig. 1(d) due to the nonvanishing $\delta_{\mathrm{JT}}^{(i)}$. The origin of this disagreement is unknown and beyond the scope of this work. We suggest that it may represent an energy-resolution limitation in the approach employed. We note that inclusion of higher-order terms[40] up to fourth order in electron-phonon interactions is found to negligibly change our results.

The coupled spin-vibronic results are shown in the final panel of Fig. 2(d) and are found after including the SOC Hamiltonian directly. We find that the $m_s = 0$ and $m_s = \pm 1$ sublevels of the A_{2u} vibronic states are split, in the case of SnV^0 by 5.9 meV. The $m_s = \pm 1$ sublevels of the E_u states also split (here we distinguish the E_u states by labels + and −). These $E_u^{\pm}$ states have a Kramers degeneracy, very much analogous to the lowest E_g vibronic states of the group IV^-, where $|^3E_u^+\rangle \otimes |\uparrow\uparrow\rangle$ and $|^3E_u^-\rangle \otimes |\downarrow\downarrow\rangle$ are the degenerate, lowest energy E_u states. These are split by an energy of $\lambda_u + \lambda_g$ from the degenerate $|^3E_u^-\rangle \otimes |\uparrow\uparrow\rangle$ and $|^3E_u^+\rangle \otimes |\downarrow\downarrow\rangle$ states, as shown in Fig. 2(d) for SnV^0. In the absence of JT interactions this splitting $\lambda_g + \lambda_u$ would be over 100 meV, however here it is only ~ 3 meV, a direct consequence of the strong electron-phonon coupling present in the pJT system. Additional interactions such as effects of strain and spin-spin coupling could split and shift these levels further.

For all cases, the reduction factors denoted by $p_{u/g}$ are smaller than 0.05, indicative of a very strong quenching of the SO interaction, even more so than the group IV^- color centers. This can be attributed in part to the scaling of the Jahn-Teller instability vs. the spin-orbit splitting in the two-hole case. While to first order the JT energy scales as the square of the coupling (i.e., $\sim (F_u + F_g)^2$), the SO splitting scales linearly (i.e., $\lambda_g + \lambda_u$). Such a scaling and the resulting JT energies intuitively explains the significant SO quenching we find in this work. We note that shifts in

the absolute energies of the E_u states are found to be most significant in the case of PbV^0, where we find a redshift in the predicted ZPL of roughly 0.05 eV. All lighter defects have much weaker absolute energy shifts due to their reduced SO coupling constants.

In conclusion, we present first principles calculations of group IV neutral artificial atoms in diamond, where we capture the product Jahn-Teller effect to second order in electron-phonon coupling and non-perturbatively describe the effects of spin-orbit interactions. Our results find significant reduction in the spin-orbit splitting due to the strong pJT. However, we also find that the spin-orbit interactions would split the lowest optically-active states into m_s-resolved levels split by up to a few meV in the heavier candidates. These results provide qualitatively new insight into the physics of artificial atom qubits in diamond and are of quantitative importance in experimental identification and manipulation of these centers in quantum information science.

ACKNOWLEDGMENTS

The authors thank Dr. Tomáš Neuman and Prof. Marko Lončar, at Harvard University, for helpful discussions.

This work was supported by the DOE 'Photonics at Thermodynamic Limits' Energy Frontier Research Center under grant number DE-SC0019140. D. E. and P.N. are partially supported by the Army Research Office MURI (Ab-Initio Solid-State Quantum Materials) grant number W911NF-18-1-0431 and by the STC Center for Integrated Quantum Materials (CIQM) under NSF grant number DMR-1231319. This research used resources of the National Energy Research Scientific Computing Center, a DOE Office of Science User Facility supported by the Office of Science of the U.S. Department of Energy under Contract No. DE-AC02-05CH11231. Additional calculations were performed using resources from the Department of Defense High Performance Computing Modernization program as well as resources at the Research Computing Group at Harvard University. J. F. acknowledges partial financial support from the Deutsche Forschungsgemeinschaft (DFG) under contract No. FL 997/1-1. The Flatiron Institute is a division of the Simons Foundation. P.N. is a Moore Inventor Fellow.

* These authors contributed equally
† prineha@seas.harvard.edu

[1] M. Atatüre, D. Englund, N. Vamivakas, S.-Y. Lee, and J. Wrachtrup, Nature Reviews Materials **3**, 38 (2018).
[2] D. D. Awschalom, R. Hanson, J. Wrachtrup, and B. B. Zhou, Nature Photonics **12**, 516 (2018).
[3] I. Aharonovich, D. Englund, and M. Toth, Nature Photonics **10**, 631 (2016).
[4] L. J. Rogers, K. D. Jahnke, T. Teraji, L. Marseglia, C. MÃijller, B. Naydenov, H. Schauffert, C. Kranz, J. Isoya, L. P. McGuinness, and F. Jelezko, Nature Communications **5**, 4739 (2014).
[5] J. R. Weber, W. F. Koehl, J. B. Varley, A. Janotti, B. B. Buckley, C. G. Van de Walle, and D. D. Awschalom, Proceedings of the National Academy of Sciences of the United States of America **107**, 8513 (2010).
[6] N. Kalb, A. A. Reiserer, P. C. Humphreys, J. J. W. Bakermans, S. J. Kamerling, N. H. Nickerson, S. C. Benjamin, D. J. Twitchen, M. Markham, and R. Hanson, Science **356**, 928 (2017).
[7] P. C. Humphreys, N. Kalb, J. P. J. Morits, R. N. Schouten, R. F. L. Vermeulen, D. J. Twitchen, M. Markham, and R. Hanson, Nature **558**, 268 (2018).
[8] M. W. Doherty, N. B. Manson, P. Delaney, F. Jelezko, J. Wrachtrup, and L. C. L. Hollenberg, Physics Reports The nitrogen-vacancy colour centre in diamond, **528**, 1 (2013).
[9] F. Rozpędek, R. Yehia, K. Goodenough, M. Ruf, P. C. Humphreys, R. Hanson, S. Wehner, and D. Elkouss, Physical Review A **99**, 052330 (2019).
[10] L. J. Rogers, K. D. Jahnke, M. W. Doherty, A. Dietrich, L. P. McGuinness, C. Müller, T. Teraji, H. Sumiya, J. Isoya, N. B. Manson, and F. Jelezko, Physical Review B **89**, 235101 (2014).
[11] C. Hepp, T. Müller, V. Waselowski, J. N. Becker, B. Pingault, H. Sternschulte, D. Steinmüller-Nethl, A. Gali, J. R. Maze, M. Atatüre, and C. Becher, Physical Review Letters **112**, 036405 (2014), 1310.3106.
[12] M.-A. Lemond, S. Meesala, A. Sipahigil, M. J. A. Scheutz, M. D. Lukin, M. Loncar, and P. Rabl, Physical Review Letters **120**, 213603 (2018).
[13] R. E. Evans, M. K. Bhaskar, D. D. Sukachev, C. T. Nguyen, A. Sipahigil, M. J. Burek, B. Machielse, G. H. Zhang, A. S. Zibrov, E. Bielejec, H. Park, M. Lončar, and M. D. Lukin, Science **362**, 662 (2018).
[14] D. D. Sukachev, A. Sipahigil, C. T. Nguyen, M. K. Bhaskar, R. E. Evans, F. Jelezko, and M. D. Lukin, Physical Review Letters **119**, 223602 (2017).
[15] Y. N. Palyanov, I. N. Kupriyanov, Y. M. Borzdov, and N. V. Surovtsev, Scientific Reports **5** (2015), 10.1038/srep14789.
[16] P. Siyushev, M. H. Metsch, A. Ijaz, J. M. Binder, M. K. Bhaskar, D. D. Sukachev, A. Sipahigil, R. E. Evans, C. T. Nguyen, M. D. Lukin, P. R. Hemmer, Y. N. Palyanov, I. N. Kupriyanov, Y. M. Borzdov, L. J. Rogers, and F. Jelezko, Physical Review B **96** (2017), 10.1103/PhysRevB.96.081201.
[17] J.-W. Fan, I. Cojocaru, J. Becker, I. V. Fedotov, M. H. A. Alkahtani, A. Alajlan, S. Blakley, M. Rezaee, A. Lyamkina, Y. N. Palyanov, Y. M. Borzdov, Y.-P. Yang, A. Zheltikov, P. Hemmer, and A. V. Akimov, ACS Photonics **5**, 765 (2018).
[18] M. K. Bhaskar, D. D. Sukachev, A. Sipahigil, R. E. Evans, M. J. Burek, C. T. Nguyen, L. J. Rogers, P. Siyushev, M. H. Metsch, H. Park, F. Jelezko, M. Lončar, and M. D. Lukin, Physical Review Letters **118**, 223603 (2017).
[19] T. Iwasaki, Y. Miyamoto, T. Taniguchi, P. Siyushev, M. H. Metsch, F. Jelezko, and M. Hatano, Physical Review Letters **119** (2017), 10.1103/PhysRevLett.119.253601.
[20] M. E. Trusheim, B. Pingault, N. H. Wan, M. GÃijndoÄ§an, L. De Santis, R. Debroux, D. Gangloff, C. Purser, K. C. Chen, M. Walsh, J. J. Rose, J. N. Becker, B. Lienhard, E. Bersin, I. Pa-

radeisanos, G. Wang, D. Lyzwa, A. R.-P. Montblanch, G. Malladi, H. Bakhru, A. C. Ferrari, I. A. Walmsley, M. AtatÃijre, and D. Englund, Physical Review Letters **124**, 023602 (2020).
[21] A. E. Rugar, C. Dory, S. Sun, and J. VuÄŊkoviÄĞ, Physical Review B **99**, 205417 (2019).
[22] J. GÃűrlitz, D. Herrmann, G. Thiering, P. Fuchs, M. Gandil, T. Iwasaki, T. Taniguchi, M. Kieschnick, J. Meijer, M. Hatano, A. Gali, and C. Becher, New Journal of Physics (2019), 10.1088/1367-2630/ab6631.
[23] M. E. Trusheim, N. H. Wan, K. C. Chen, C. J. Ciccarino, J. Flick, R. Sundararaman, G. Malladi, E. Bersin, M. Walsh, B. Lienhard, H. Bakhru, P. Narang, and D. Englund, Physical Review B **99**, 075430 (2019).
[24] S. Ditalia Tchernij, T. Lühmann, T. Herzig, J. Küpper, A. Damin, S. Santonocito, M. Signorile, P. Traina, E. Moreva, F. Celegato, S. Pezzagna, I. P. Degiovanni, P. Olivero, M. Jakišić, J. Meijer, P. M. Genovese, and J. Forneris, ACS Photonics **5**, 4864 (2018).
[25] B. L. Green, M. W. Doherty, E. Nako, N. B. Manson, U. F. S. D'Haenens-Johansson, S. D. Williams, D. J. Twitchen, and M. E. Newton, Physical Review B **99**, 161112 (2019).
[26] B. L. Green, S. Mottishaw, B. G. Breeze, A. M. Edmonds, U. F. S. DâĂŹHaenens-Johansson, M. W. Doherty, S. D. Williams, D. J. Twitchen, and M. E. Newton, Physical Review Letters **119**, 096402 (2017).
[27] B. C. Rose, D. Huang, Z.-H. Zhang, P. Stevenson, A. M. Tyryshkin, S. Sangtawesin, S. Srinivasan, L. Loudin, M. L. Markham, A. M. Edmonds, D. J. Twitchen, S. A. Lyon, and N. P. d. Leon, Science **361**, 60 (2018).
[28] G. Thiering and A. Gali, Physical Review X **8**, 021063 (2018).
[29] G. Thiering and A. Gali, npj Computational Materials **5**, 18 (2019).
[30] I. Harris, C. J. Ciccarino, J. Flick, D. R. Englund, and P. Narang, arXiv:1907.12548 (2019).
[31] P. Narang, C. J. Ciccarino, J. Flick, and D. Englund, Advanced Functional Materials **29**, 1904557 (2019).
[32] I. Bersuker and V. Polinger, *Vibronic Interactions in Molecules and Crystals*, Vol. 49 (Springer Series in Chemical Physics, Springer-Verlag Berlin, Heidelberg, 1990).
[33] Q.-c. Qiu, Frontiers of Physics in China **2**, 51 (2007).
[34] Q. C. Qiu, L. F. Chibotaru, and A. Ceulemans, Physical Review B **65**, 035104 (2001).
[35] I. B. Bersuker, Journal of Physics: Conference Series **833**, 012001 (2017).
[36] G. Kresse and J. Furthmüller, Physical Review B **54**, 11169 (1996).
[37] F. S. Ham, Physical Review **138**, A1727 (1965).
[38] G. Thiering and A. Gali, Physical Review B **96**, 081115 (2017).
[39] C. Hepp, *Electronic Structure of the Silicon Vacancy Color Center in Diamond*, Ph.D. thesis, Saarland University (2014).
[40] A. Viel and W. Eisfeld, The Journal of Chemical Physics **120**, 4603 (2004).